Physics Insight of the Inertia of Power Systems and Methods to Provide Inertial Response

Yongzhang Huang, *Member*, *IEEE*, Yuxuan Wang, Chenyang Li, Haisen Zhao, *Senior Member*, *IEEE*, and Qianyu Wu

***Abstract*—The growth of renewable energy reduces the moment of inertia for the synchronous AC grid, so the authors put forward two basic questions: 1) What is the physics insight that a synchronous AC grid needs for mechanical inertia? 2) How to provide inertial response for the power grid dominated with renewable energy? Based on Einstein's special relativity and the Lorentz transformation, these papers illustrates that the nature of the inertia of the AC grid comes from the relativity of the electromagnetic field and motion, and from the strong coupling between them. According to their nature, the inertial response of the synchronous generator is self-proven. By contrast, the converter for the grid-connection of renewable energies used various algorithms in order to provide virtual inertia. But because algorithms do not rebuild the coupling between electromagnetic fields and motion, it is doubtful whether they can provide inertia and inertial responses. Therefore, the authors propose that there is a need to build extra electromagnetic fields and motion coupling for grids with high penetration rates of renewable energy. Therefore, a new grid-connection technology via Motor-Generator Pair (MGP) is discussed. The electromagnetic-motion coupling of the MGP is analyzed, and the results of simulation and experimental studies are also reported.**

***Index Terms*—Electromagnetic-motion coupling, inertia response of power systems, Lorentz transformation, motor-generator pair (MGP), power systems with high proportion of renewable energy.**

I. INTRODUCTION

THE Chinese government undertakes to adopt effective measures to reach peak carbon emissions by 2030 and carbon neutrality by 2060, triggering a need for sharply increasing the proportion of renewable energy in power generation systems according to the estimates made by relevant departments and power companies, that is, the power systems with high proportion of renewable energy will become a reality. Under this background, the power systems based on conventional synchronous generators (SGs) are gradually evolving to those with a high proportion of renewable energy, such as wind and photovoltaics [1], [2]. The traditional grid and SGs follow the power angle equations and their behavior are well understood. Unfortunately, the grid and converter-connected renewable energy do not follow power angle equations. For example, in the case of an active power disturbance, renewable energy cannot actively provide inertia support for power systems. As a result, with the increase of the proportion of renewable energy, the total inertia level will decrease, and the system frequency stability will gradually deteriorate. The weakening of system stability due to insufficient inertial support often occurs throughout the world. In severe cases, it will lead to a sudden drop in frequency and further to the grid-disconnection of renewable energy [3], [4]. Therefore, weak inertia is one of the instability concerns with a high proportion of renewable energy.

A lot of studies have been done worldwide as to how to provide wind turbines and photovoltaics with inertia, however, the results are not promising. The approaches include current source converter control and voltage source converter control [5]. The former introduces the change of the grid frequency into the outer loop of active power control and inverters can release the kinetic energy stored from the rotors of wind turbines or stored energy from batteries in a short time period, so as to quickly respond to the transient change of grid frequency and to provide the moment of inertia similar to that of SGs [6]. However, this method could not produce the inertia response which SGs can, it only changes the output power according to the direction of the frequency change to compensate for the power imbalance of the system. This is essentially a fast primary frequency regulation. Additionally, converters are lacking the power sharing features of SGs. At the moment of load power disturbance, SGs can instantaneously share the unbalanced power according to their locations and capacities based on the Lenz Law. The Virtual Synchronous Generator (VSG) technology [7] is the representative of voltage source control, which introduces the motion equation of SGs into the control algorithm of converters to mimic the inertial response. Although in theory, converters with VSG control may have power sharing, they are unable to mimic the electromagnetic and motion coupling of SGs, therefore the large unbalanced torque in transient state could affect the operations of renewable energy farms. So far, the VSG control essentially functions as a fast primary frequency regulation [8].

Looking at the frequency drop curve in the transient state, the mechanical inertia of the SG rotor helps to reduce the drop rate and drop depth. As stated in the textbook of power systems, the system frequency is characterized by the

Manuscript received November 22, 2021, accepted December 23, 2021. Date of online publication January 5, 2022, date of current version February 16, 2022.

Y. Z. Huang, Y. X. Wang, C. Y. Li, H. S. Zhao, and Q. Y. Wu (corresponding author, e-mail: m18810663690_1@163.com) are with the State Key Laboratory for Alternate Electrical Power System with Renewable Energy Sources, North China Electric Power University, Beijing 102206, China.

DOI: 10.17775/CSEEJPES.2021.08670

2096-0042 © 2021 CSEE

rotor rotation speed of SG. According to Faraday's law of electromagnetic induction, the frequency of the AC voltage and current generated by SG is also the rotational frequency of the rotor, thus the motion of the rotor correlates the rotor frequency with the power imbalance of the power system. This causes the frequency to become the characteristic indicator of power imbalance. The SG is the cornerstone of power system, and the mechanical inertia of its rotor plays a key role in the frequency stability of the power system.

On the one hand, the stable operation of the synchronous AC grid depends on the mechanical inertia of the SG. On the other hand, renewable energy reduces the total number of SGs. So far, it remains unclear whether the grid-connected converter can provide inertia by its circuit topology and control algorithms. Therefore, the authors put forward two basic questions: 1) What is the physics insight that a synchronous AC grid needs for mechanical inertia? 2) How to provide inertial for the power grid dominated with renewable energy? These two questions need to be answered theoretically.

This paper attempts to answer the above two questions from the perspective of the electromagnetic field and motion (EM-motion) coupling. Section II introduces the inertia and inertial response of the power system based on the traditional theory of synchronous generators. Section III attempts to answer a neglected but very fundamental question, why there exists the mechanical moment of inertia and why it still plays a key role in today's synchronous AC grid which has been evolving for more than a hundred years. To answer this question, the authors review Faraday's law of electromagnetic induction and Einstein's classic articles in establishing his special relativity [9]. Einstein applied Lorentz's transformation to the classical Maxwell's electromagnetic equation, thereby revealing that Maxwell's equations obey the relativity principle. Lorentz transformation reveals the relativity of the electromagnetic field and motion, and the close coupling between them. According to the physical structure and operation principle of three phase SG, the authors draw a basic conclusion that the nature of the inertia response of synchronous AC power systems originates from Lorentz's transformation, that is, the EM-motion coupling. Section IV describes the equipment that traditionally are capable of providing inertia response, such as SGs and condensers, both of which are processes of EM-motion coupling. In Section V, the authors express concern that EM-motion coupling does not exist due to the lack of motion in the converter-based grid-connection technology. Furthermore, the control algorithms aimed to provide virtual inertia do not add motion or rebuild the EM-motion coupling. It is therefore inferred that converters may not be capable of providing inertial response, but may only be capable of supplementing power to realize faster primary frequency regulation. In order to rebuild the EM-motion coupling, Section VI introduces a new way of grid-connection for renewable energy through Motor-Generator Pair (MGP), the structure of MGP and its EM-motion coupling, and the analysis of the inertial response from MGP based on these coupling characteristics. In Section VII, simulation and experiments demonstrate that the inertial response introduced by the MGP helps to improve the frequency stability of power systems.

II. Physics Insight of Inertia in Power Systems

A. *Classification of Inertia in Power Systems*

In physics, inertia is an inherent attribute of objects. For a rotating object, inertia means that it has an inherent attribute of maintaining static or uniform rotation, which is characterized by the resistance of the object to the change of its rotation state. The moment of inertia J is a measure of inertia when an object rotates about an axis, which is given by:

$$J = \int r^2 \mathrm{d}m \tag{1}$$

where r is the radius of rotation, and m is the mass of the rotating object.

In a synchronous generator, the relationship between the speed ω_r of a rotating object and its driving mechanical torque T_{M} and braking electromagnetic torque T_{E} can be expressed as:

$$J\frac{\mathrm{d}\omega_r}{\mathrm{d}t} = T_{\mathrm{M}} - T_{\mathrm{E}} \tag{2}$$

The change of speed ω_r with time can be expressed as:

$$\omega_r = \omega_{rt_0} + \frac{1}{J}\int_{t_0}^{t}(T_{\mathrm{M}} - T_{\mathrm{E}})\mathrm{d}t \tag{3}$$

where t_0 is the initial time and ω_{t0} is the speed at t_0.

It can be seen from (3) that when the torque suddenly changes, the speed of the object does not abruptly change due to the inertia of the object itself, but continuously transits from the initial speed to another speed. The speed of this process is affected by the moment of inertia.

The rotational energy E_r stored by an object rotating at ω_r can be expressed as:

$$E_r = \int J\frac{\mathrm{d}\omega_r}{\mathrm{d}t}\omega_r \mathrm{d}t = \frac{1}{2}J\omega_r^2 \tag{4}$$

In the electromagnetic field, the elements that store the magnetic field energy and electric field energy are inductors and capacitors respectively. According to the law of electromagnetic induction, the current i_{L} flowing through an inductor can be given by:

$$L\frac{\mathrm{d}i_{\mathrm{L}}}{\mathrm{d}t} = \Delta u_{\mathrm{L}} \tag{5}$$

where L is the inductance, and u_{L} is the voltage across the inductor.

The change of inductive current i_{L} with time can be expressed as:

$$i_{\mathrm{L}} = i_{\mathrm{L}t_0} + \frac{1}{L}\int_{t_0}^{t} u_{\mathrm{L}}\mathrm{d}t \tag{6}$$

where $i_{\mathrm{L}t_0}$ is the inductive current at t_0.

Equation (6) shows that the current flowing through the inductor does not change abruptly with the presence of L. The magnetic field energy E_{L} stored by the inductor is expressed as:

$$E_{\mathrm{L}} = \int L\frac{\mathrm{d}i_{\mathrm{L}}}{\mathrm{d}t}i_{\mathrm{L}}\mathrm{d}t = \frac{1}{2}Li_{\mathrm{L}}^2 \tag{7}$$

The voltage u_{C} across the capacitor can be given by:

$$C\frac{\mathrm{d}u_{\mathrm{C}}}{\mathrm{d}t} = \Delta i_{\mathrm{C}} \tag{8}$$

where, C is the capacitance, and i_{C} is the current flowing through the capacitor.

The change of voltage u_{C} with time can be expressed as:

$$u_{\mathrm{C}} = u_{\mathrm{C}t_0} + \frac{1}{C}\int_{t_0}^{t} i_{\mathrm{c}}\mathrm{d}t \tag{9}$$

where, $u_{\mathrm{C}t_0}$ is the voltage across the capacitor at t_0.

Equation (9) shows that the voltage across the capacitor does not abruptly change. The electric field energy E_{C} stored by the capacitor is expressed as:

$$E_{\mathrm{C}} = \int C\frac{\mathrm{d}u_{\mathrm{C}}}{\mathrm{d}t}u_{\mathrm{C}}\mathrm{d}t = \frac{1}{2}Cu_{\mathrm{C}}^2 \tag{10}$$

To sum up, the inertia in power systems is divided into mechanical inertia and electromagnetic inertia, as shown in Table I. The structure and operation principle of the synchronous motor determines the existence of both mechanical inertia and electromagnetic inertia which provide resistance to the changes of physical quantities such as current, voltage and rotation speed when the system is disturbed.

B. Inertial Response of the Synchronous Generator

The equation of SG's rotor motion is the key in analyzing the frequency stability of the power system, which describes the influence of electromagnetic power P_{e} and mechanical power P_{m} on the speed ω of the rotor, then it can be expressed in per unit value as:

$$2H\frac{\mathrm{d}\omega}{\mathrm{d}t} = P_{\mathrm{m}} - P_{\mathrm{e}} - K_{\mathrm{D}}\omega \tag{11}$$

where H is the time constant of SG's inertia, which is only related to the moment of inertia J for running at rated speed; K_{D} is the damping coefficient.

The active power transmitted from the SG to the load is expressed as:

$$P_{\mathrm{e}} = \frac{E_{\mathrm{G}}'U_{\mathrm{L}}}{X_{\mathrm{T}}}\sin\delta \tag{12}$$

where E_{G}' is the internal electrical potential of the SG, U_{L} is the voltage at the load, X_{T} is the equivalent reactance between E_{G}' and U_{L}, and δ is the phase angle difference between E_{G}' and U_{L}.

In the equivalent circuit model, the E_{G}' of the SG is given by:

$$E_{\mathrm{G}}' = \frac{X_{\mathrm{ad}}}{X_f}\psi_f = \frac{X_{\mathrm{ad}}}{X_f}(-X_{\mathrm{ad}}i_{\mathrm{d}} + X_f i_f) \tag{13}$$

where ψ_f is rotor flux, X_{ad} is mutual inductive reactance of stator d-axis winding and rotor winding, X_f is rotor winding reactance, i_{d} is stator d-axis current, and i_f is rotor winding current.

Immediately after power disturbance, the inertial response of the SG can be divided into two stages. The first stage features the electromagnetic power sharing, the SGs instantaneously share the system power imbalance at the moment of disturbance, and even more remarkable is that the amount of power sharing by a specific SG is proportional to its capacity (proportional to its electromagnetic inertia) and its distance to the disturbance point; The second stage features the mechanical power sharing, the mechanical energy stored in the rotor is converted into electromagnetic power to cut the deficit of the imbalanced system power, the amount of sharing is proportional to its mechanical inertia. The second stage will reduce the frequency drop depth and drop rate. The phenomenon in these two stages is so-called electromagnetic-mechanical coupling named by the industry.

Equation (11) is not only suitable for steady state, but also for the above transient state. When there is an abrupt change in the grid, in order to solve (11) to get transient frequency variation, the initial condition at the disturbance moment must be known. That initial condition is just the result of electromagnetic power sharing described above.

The phasor diagram Fig. 1 depicts how to determine transient initial conditions according to the physics law. Taking the increase of load power as an example, the electromagnetic inertia of the inductor prevents i_{d} and i_f from abruptly changing at the moment of disturbance, thereby preventing the rotor flux ψ_f and the amplitude of internal electrical potential E_{G}' of SGs from doing so. According to Lenz's law, the current I in the line suddenly changes to I' after the load increase. At the moment of disturbance, the inertia of rotor speed prevents the phase of E_{G}' from abruptly changing, and the surge of current I in the circuit makes the phase angle difference δ_{L} between E_{G}' and U_{L} instantaneously widen to δ_{L}' Put δ_{L}' to (12), find that the electromagnetic power of the synchronous generator instantaneously increases to share the increase of the disturbance power.

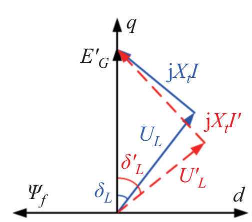

Fig. 1. Schematic phasor diagram of physics variables of SGs at the moment of abrupt load power increase.

TABLE I
CLASSIFICATION OF INERTIA IN POWER SYSTEMS

Name of inertia	Mechanical inertia	Electromagnetic inertia	Electromagnetic inertia
Physical carrier with inertia	Moment of inertia J	Capacitance C	Inductance L
Characteristic physical variables of inertia	Rotational speed ω_r	Voltage u_{C}	Current i_{L}
Inertial energy of carrier	Mechanical energy $\frac{1}{2}J\omega_r^2$	Electric field energy $\frac{1}{2}Cu_{\mathrm{C}}^2$	Magnetic field energy $\frac{1}{2}Li_{\mathrm{L}}^2$
Equation characterizing inertia	$J\frac{\mathrm{d}\omega_r}{\mathrm{d}t} = T_{\mathrm{M}} - T_{\mathrm{E}}$	$C\frac{\mathrm{d}u_{\mathrm{C}}}{\mathrm{d}t} = \Delta i_{\mathrm{C}}$	$L\frac{\mathrm{d}i_{\mathrm{L}}}{\mathrm{d}t} = \Delta u_{\mathrm{L}}$

Given the above initial power shared, (11) can characterize the subsequent changes. When the electromagnetic power of SG increases, the mover could not catch up to this fast change. Under the unbalanced torque, the speed of the SG's rotor decreases to release its kinetic energy to supplement the imbalance of system power. This process is referred to as the mechanical inertial response of the SG, the SG can release its mechanical energy at the right time to ease the power imbalance.

In power systems, the relationship between the mechanical energy of the rotor and the output electromagnetic power of the SG is described in (11), including finding the initial conditions in transient state, is generally is expressed as the EM-motion coupling. The next section discusses the physics insight of this coupling.

III. Physics Insight of Inertia in Power Systems

Faraday's law of electromagnetic induction shows that the change of magnetic flux can produce an electric field. Maxwell ingeniously put forward the hypothesis of displacement current, thereby establishing a complete classical electromagnetic theory. He then predicted the electromagnetic wave and calculated its propagation speed which was the same as the speed of light. Maxwell's equations are expressed as:

$$\begin{cases} \nabla \times \boldsymbol{B} = \mu_0 \left(\boldsymbol{J} + \varepsilon_0 \frac{\partial \boldsymbol{E}}{\partial t} \right) \\ \nabla \times \boldsymbol{E} = -\frac{\partial \boldsymbol{B}}{\partial t} \\ \nabla \cdot \boldsymbol{B} = 0 \\ \nabla \cdot \boldsymbol{E} = \frac{\rho}{\varepsilon_0} \end{cases} \tag{14}$$

where $\boldsymbol{E}$ is the electric field intensity, $\boldsymbol{B}$ is the magnetic induction intensity, $\boldsymbol{J}$ is the current density, μ_0 is the vacuum permeability, ρ is the charge density, and ε_0 is the permittivity of vacuum.

Faraday's law of electromagnetic induction is accurately described as the induced electric field resulting from the change of flux, while flux change can be realized by the motion of either coil or magnet, so that Faraday's law of electromagnetic induction is related to motion. In history, researchers had found Faraday's law has two phenomena. Fig. 2 shows a simple thought experiment about these two phenomena.

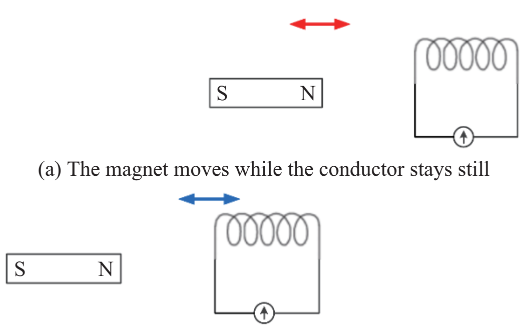

(a) The magnet moves while the conductor stays still

(b) The conductor moves while the magnet stays still

Fig. 2. Thought experiment of the motion of magnet and coil.

In Fig. 2(a), the magnet is moving while the conductor stays still, an electric field is generated near the magnet, and a current is generated in the conductor due to the induced electric field. In Fig. 2(b), the magnet is stationary while the conductor is moving, no electric field is generated near the magnet, but a current is generated in the conductor due to the induced electric field. The relative positions of magnet and coil are the same in both cases, but with the only differences in motion, resulting in the asymmetry of electric field and magnetic field. This experiment shows not only the electromagnetic-motion correlation, but also the incompatibility between Newton's classical mechanics and Maxwell's classical electromagnetic theory. Under Galileo transformation of classical mechanics, the electromagnetic theory does not obey the principle of relativity, or the principle of coordinate invariance.

Many physicists have made interpretative explanations on the two phenomena. Even the great theoretic physicists, such as Lorentz, although as found by the Lorentz transformation, he could not abandon the absolute space-time view of Newtonian mechanics. Lorentz's transformation is shown in (15).

$$\begin{aligned} t' &= \gamma \left(t - \frac{vx}{c^2} \right) \\ x' &= \gamma (x - vt) \\ y' &= y \\ z' &= z \end{aligned} \tag{15}$$

where x, y, z and x', y', z' are the axes of two coordinate systems, t and t' are the time in the corresponding coordinate systems, v is the speed of relative movement between coordinate systems, and c is the speed of light. $\gamma = (\sqrt{1 - v^2/c^2})^{-1}$.

Lorentz's explanation of Lorentz transformations was about interpreting physical phenomena through some mathematic tricks. But he did not reflect their physics significance with the relativistic view of time and space.

In 1905, Einstein published his "*On the Electrodynamics of Moving Bodies*" [9]. Though this paper marked the birth of a brand-new view of time and space (special relativity), he used nearly half the paper discussing the relativity of the electric field, magnetic field and their motion, that is, the EM-motion coupling used by the authors. At the beginning of the article, Einstein described the asymmetry caused by motion shown in the thought experiment in Fig. 2.

For the vector of the electric field and magnetic field, the Lorentz transformation is expressed as:

$$\begin{aligned} \boldsymbol{E'}_{//} &= \boldsymbol{E}_{//} \\ \boldsymbol{B'}_{//} &= \boldsymbol{B}_{//} \\ \boldsymbol{E'}_{\perp} &= \gamma (\boldsymbol{E}_{\perp} + \boldsymbol{V} \times \boldsymbol{B}) \\ \boldsymbol{B'}_{\perp} &= \gamma \left(\boldsymbol{B}_{\perp} - \frac{\boldsymbol{V}}{\boldsymbol{c}^2} \times \mathrm{E} \right) \end{aligned} \tag{16}$$

where $\boldsymbol{E}$ is the electric field in the rest system, $\boldsymbol{E'}$ is the electric field in the moving system, $\boldsymbol{B}$ is the magnetic field in the rest system, $\boldsymbol{B'}$ is the magnetic field in the moving system, and $\boldsymbol{V}$ is the velocity of the moving system relative to the rest system. The subscripts $//$ and $\perp$ are the parallel and perpendicular components to the direction of motion of the moving system relative to the rest system, respectively.

Under the Lorentz transformation, Maxwell's equations are the same in different inertial frames, that is, electromagnetic phenomena obey the principle of relativity. Einstein wrote: "the same laws of electrodynamics and optics will be valid for all frames of reference for which the equations of mechanics hold good."

It is evident from (16) of the Lorentz transformation that if either electric field or magnetic field does not exist in a rest system, for instance, $\boldsymbol{E}$ or $\boldsymbol{B}$ is 0, but the electric field or magnetic field may present in a moving system, i.e., $\boldsymbol{E}'$ or $\boldsymbol{B}'$ is not 0. Therefore, electricity and magnetism are relative and not independent of the motion state of the reference system. In other words, the electric field, magnetic field and motion are directly coupled.

For the asymmetry shown in the experiment in Fig. 2, Einstein explained with Lorentz transformation: "If a unit electric point charge is in motion in an electromagnetic field, the force acting upon it is equal to the electric force which is present at the locality of the charge, and which we ascertain by transformation of the field to a system of co-ordinates at rest relatively to the electrical charge." "Electric and magnetic forces do not exist independently of the state of motion of the system of co-ordinates. Furthermore, it is clear that the asymmetry mentioned in the introduction as arising when we consider the currents produced by the relative motion of a magnet and a conductor, now disappears."

For a synchronous AC grid based on SG, its EM-motion coupling is deeply rooted in Einstein's special relativity and is clearly expressed by the Lorentz transformation. Therefore, the authors draw a basic conclusion that the inertia response of synchronous AC grid originates from the Lorentz transformation, in other words, from EM-motion coupling.

In the past, high-speed moving elementary particles are used as examples to calculate the clock slow down or the length contraction in order to understand special relativity. Now, the special relativity exists directly in the synchronous AC grid. This relativity (coupling) among electricity, magnetism and motion plays a great role in stable operation of the synchronous AC grid.

IV. Methods to Increase Inertia Based on the EM-Motion Coupling

Section II describes the inertia and inertial response of SGs, and Section III explains the physics insight of SG's inertia from the perspective of EM-motion coupling. Based on the nature of inertia and the operation practice of the power grid, the authors derive the first hypothesis that the inertial response required by the synchronous AC grid can only be provided by equipment with EM-motion coupling.

A synchronous condenser is a synchronous motor with no-load operation, of which the reactive power compensation is essentially realized through the EM-motion coupling. Therefore, condensers can obviously be used also to increase the inertia in power systems.

Condensers have been used as the main reactive power compensation equipment since the 1950s, but are gradually being replaced by power electronics based reactive compensation due to no-load loss and maintenance costs.

Because of the large-scale feed from the HVDC transmission, the problem of insufficient reactive power support is becoming increasingly severe. This introduces the resumption of condensers in power systems from the beginning of the 21 st century. The engineering practice in China shows that the transient process related to HVDC transmission is very short, and power electronic compensation equipment with inherent time delay may worsen the system characteristics and produce a "counter regulation" effect [10] when the voltage of the converter station rapidly changes as in the case of commutation failure and HVDC block in the sending-end. Due to the intrinsic EM-motion coupling and the strong short-term overload capacity, condensers provide faster and stronger dynamic reactive power support. For example, the 2×300 Mvar Condensers at Shaoshan Converter Station in Hunan Province is China's first condenser project put into operation at the receiving-end of the HVDC line. Its reactive compensation capability is 2–3 times that of static synchronous compensators (STATCOM), which effectively improves the operation capability and voltage stability of the HVDC line. With further improvements in structure and parameters design, condensers can play a better role in reactive power support in the future [11].

In recent years, some engineering projects abroad have also demonstrated that condensers can provide not only fast reactive compensation, but also the inertia support for weak grids. For example, high-inertia condensers have been deployed to improve the frequency support for the Newfoundland power grid in St. John's, Canada. The condensers provide an inertia time constant up to 7.84 s [12], which is 6$\sim$7 times that of a normal condenser. The National Grid of the UK is implementing a hybrid condenser project in Nielston, which is expected to be completed in 2021 and intended to enhance the inertia of the grid as well as the short-circuit capacity and reactive compensation capability by installing 140 MVA rated synchronous condensers and STATCOM [13]. The excellent performance in inertia support of synchronous condensers has been demonstrated in the above engineering practices. However, there is no such practice in China as of yet.

So far, the effective equipment providing inertia for the grid is the SGs and condensers. This fact supports the first hypothesis that the inertial response required by the synchronous AC grid can only be provided by equipment with EM-motion coupling.

V. Grid-Connected Converters Lack of EM-Motion Coupling

The typical control structure of a typical grid-connected converter for renewable energy power generation is shown in Fig. 3. This principle is widely used in grid-connected PV and battery storage, and is extended to wind turbines to some degree.

Inside converters, the electric current from renewable energies is first smoothed in the capacitor, then is chopped by switches into a series of pulses, these pulses are organized by a control algorithm and are filtered by inductors into sinusoidal forms, then the sinusoidal forms are fed into the grid at the expected timing adjusted by PLL and the control algorithm. The control algorithm also uses an active and

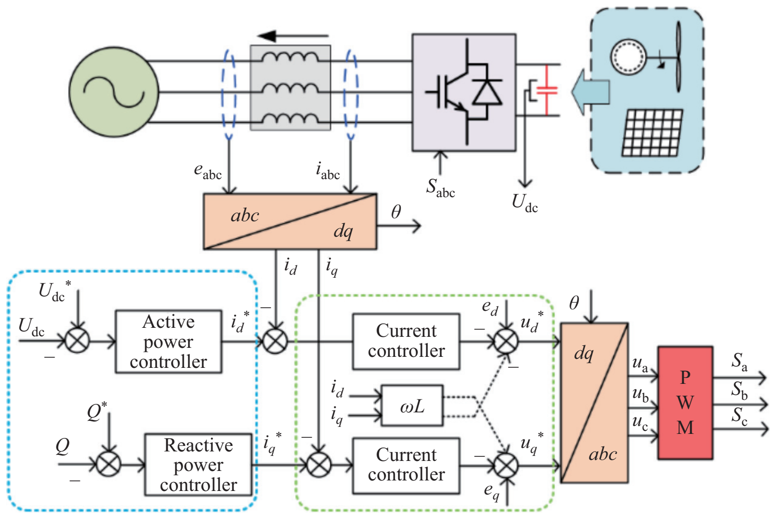

Fig. 3. Typical control loops of grid-connected converters.

reactive power control via the vector control-based coordinate transformation and voltage orientation. That is, the form and the timing of the arriving power to the grid are completely determined by control algorithms. Regardless of how dedicated the algorithm is, there is no EM-motion coupling existing between converters and the grid. Therefore, there is no inertia provided by converters. The converters cannot expect to have the features, such as power sharing and inertial response, which the SG has.

In order to add the correlation between the renewable energy operation and grid frequency, "virtual" inertia is a potential suggestion. A typical virtual inertia control is shown in Fig. 4, and the idea is to add a feedback link proportional to the change or the change rate of the system frequency on the active power control loop as shown in Fig. 3, to allow the converter to respond to the frequency variations to increase or decrease the active power output. The virtual inertia is generally sourced from the kinetic energy stored in the energy storage, such as capacitor or battery, or in the rotor of the wind turbine. The energy storage can be different but is of the same basic idea in the control.

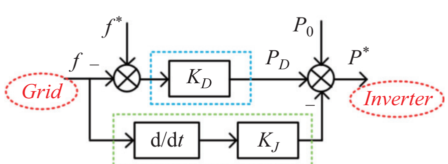

Fig. 4. Block diagram of the typical virtual inertia control.

A sensor of the converter detects the grid frequency change to initiate the output power change for frequency support, so the process lags the grid disturbances. This inherent delay makes it hard to instantaneously do the power sharing. For wind turbines, excessive use of kinetic energy stored in the rotor may also cause secondary frequency drop. For the equipment with energy storage, it provides support by fast charging and discharging. Currently there are some energy storage projects running very well and playing a role in the grid stability, such as the Energy Storage Power Station in Bordesholm, Germany, and the Hornsdale Power Reserve in Australia. However, they primarily provide primary services, such as frequency regulation, peak shaving, voltage regulation and black start [14]. Essentially, the EM-motion coupling of the SG is not presented in virtual inertia control, the SG's inertia response in transient state does not show up in the above practices.

Based on the conclusions of the physics insight of inertia, and on the fact that conventional grid-connected converters do not rebuild the EM-motion coupling for renewable energy, the authors derive their second hypothesis that the grid-connected converters may be unable to provide the inertial response required by the synchronous AC grid, but will instead supplement the unbalanced power through fast primary frequency regulation.

Generally speaking, converter based renewable energy power generation at present has no EM-motion coupling, but relies on stable grid voltage as the control reference for converters to follow the grid. For a grid with 100% penetration of renewable energy, there is a big question as to whether the grid can still provide a stable voltage and frequency reference to ensure the normal operation of converters. Till now, all the existing or in-developing algorithms of converters are essentially trying to mimic but not to rebuild the natural coupling between the electromagnetic field and motion. So, if there is no new technology to provide stable EM-motion coupling for future converters, there definitely exists a critical maximum proportion of renewable energy, which is restricted by the present converters do to their nature. Whether this maximum proportion can meet the goal of the carbon emission restriction act, will be the big question to answer. The authors suggest it is necessary to rebuild the EM-motion coupling for the electrical power produced by renewable energy.

VI. MGP Technology to Enhance Inertia of Power Systems with Renewable Energy

A. Structure and Characteristics of MGP Technology

Based on the understanding of the physics insight on EM-motion coupling in SGs and the inertial response from the mechanical inertia in SGs after power disturbance, the authors developed MGP technology [15], [16] on the foundation of synchronous machines. As shown in Fig. 5, the MGP system consists of a coaxially connected synchronous motor (SM) and synchronous generator (SG). Renewable energy, such as wind and photovoltaics, drives SM via a converter, SM drives SG and then completes the grid-integration. Unlike the popular grid-connection converters, MGP achieves the grid-connection of renewable energy through the coupling process of electrical-mechanical-electrical conversion.

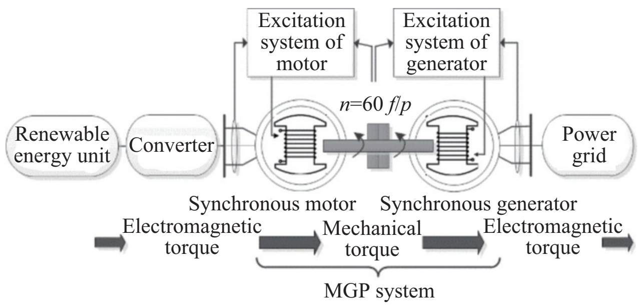

Fig. 5. Layout of MGP grid-integration.

From the physics point of view, MGP rebuilds the EM-motion coupling for renewable energy through electromechanical energy conversion, laying a solid foundation for the stable operation of the synchronous AC grid dominated with renewable energy.

The MGP system provides renewable energy farms with excellent characteristics of SGs, such as inertial response, mechanical isolation of the electrical influence between source and grid, overvoltage and overcurrent tolerance, and sufficient reactive power support for both ends of the energy farms and grid [17]. The MGP system makes full use of the EM-motion coupling, which not only retains the role of mechanical inertia, but also retains all the other characteristics of SGs. It is very likely that MGP technology is the solution to power systems with a high proportion of renewable energy. Some studies have been made on the feasibility of MGP technology, and although it has not yet been put into a practical application, it is in line with the first hypothesis of this paper.

B. EM-motion Coupling and Motion Equation of MGP

MGP rebuilds the EM-motion coupling through energy conversion. The converter modulates the coming electrical power into time varied electrical current; this current produces a rotational magnetic field in the SM, then drives the rotation of the SM's rotor and SG's rotor, thereby generating a rotating magnetic field in the SG; SG's stators pick up the varying magnetic field and produces a three-phase time varied electrical voltage and current.

The power angle characteristics of MGP are described as follows with common notations of AC theory. As shown in Fig. 6, E'_{M} and E'_{G} are the internal electrical potential of SM and SG. The SM and the SG have independent power angles δ_{M} and δ_{G} though these two angles are correlated, U_{BM} and U_{BG} are terminal voltages of SM and SG, respectively.

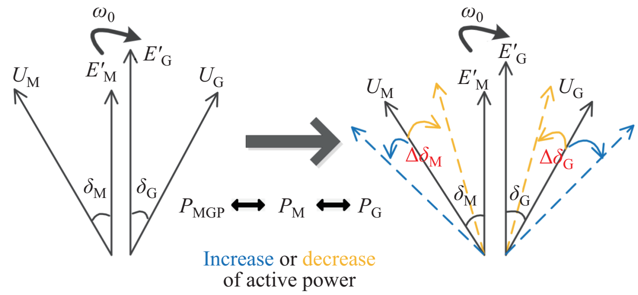

Fig. 6. Power angle characteristics of the MGP system.

Ignoring the torsional stiffness of the mechanical shafts of MGP, the rotors of SM and SG have the same angular velocity, thus E'_{M} and E'_{G} rotate synchronously at the synchronous speed ω_0. Because of mechanical loss, the power P_{M} of SM is a little larger than the power P_{G} of SG. The power angles δ_{M} and δ_{G} of MGP vary with the same tendency as the variation of P_{M} and P_{G}.

The rotors of MGP are rigidly connected, and the mechanical torque T_{mG} and angular velocity ω_{G} of the SG are equal to the mechanical torque T_{mM} and angular velocity ω_{M} of the SM, respectively. For simplicity, SM and SG are made identical in capacity and structure, they have equal inertia time constants H. Equations (17) and (18) characterize the motions of the SM and the SG respectively.

$$\begin{cases} D\Delta\omega_{\mathrm{M}} = \frac{1}{2H}(P_{\mathrm{eM}} - P_{\mathrm{mM}} - K_{\mathrm{DM}}\Delta\omega_{\mathrm{M}}) \\ D\Delta\delta_{\mathrm{M}} = \omega_0\Delta\omega_{\mathrm{M}} \end{cases} \tag{17}$$

$$\begin{cases} D\Delta\omega_{\mathrm{G}} = \frac{1}{2H}(P_{\mathrm{mG}} - P_{\mathrm{eG}} - K_{\mathrm{DG}}\Delta\omega_{\mathrm{G}}) \\ D\Delta\delta_{\mathrm{G}} = \omega_0\Delta\omega_{\mathrm{G}} \end{cases} \tag{18}$$

where D is the differential operator $\mathrm{d}/\mathrm{d}t$; $\Delta\omega_{\mathrm{M}}$ and $\Delta\omega_{\mathrm{G}}$ are the speed deviations of SM and SG respectively; K_{DM} and K_{DG} are the damping coefficients of SM and SG respectively; P_{eM} and P_{eG} are the electromagnetic torques of the SM and SG; ω_0 is the synchronous speed.

Ignoring the possible little differences in $\Delta\omega_{\mathrm{M}}$ and $\Delta\omega_{\mathrm{G}}$ related to torsional stiffness of shafts and axles in the transient state, there is, $\Delta\omega_{\mathrm{M}} = \Delta\omega_{\mathrm{G}} = \Delta\omega_r$, and equations (17) and (18) can then be simplified as:

$$\begin{cases} D\Delta\omega_r = \frac{1}{4H}[P_{\mathrm{eM}} - P_{\mathrm{eG}} - (K_{\mathrm{DM}} + K_{\mathrm{DG}})\Delta\omega_r] \\ D\Delta\delta_{\mathrm{G}} = \omega_0\Delta\omega_r \end{cases} \tag{19}$$

Comparing (19) and (11), it is obvious that the output power P_{eG} from MGP has direct coupling with the system frequency, which is exactly the EM-motion coupling in a traditional thermal power mover and SG with the grid. Therefore, MGP rebuilds the EM-motion coupling for the renewable energy.

C. Mechanical Inertia of MGP

Because of the direct EM-motion coupling, MGP can provide two-stage inertial response as mentioned in Section II-B for renewable energy grid-integration. The first stage features the electromagnetic power sharing, and the second stage features the mechanical power sharing. This inertial response immediately reduces the frequency drop depth and drop rate after the disturbance of power imbalance.

As an example, the moment of inertia of MGP can be calculated based on the actual shaft parameters of a 600 MW thermal power unit [18], which consists of four mass blocks: exciter, generator, low-pressure cylinder and high-pressure cylinder. The MGP system comprises two synchronous machines and two sets of an excitation system. The moment of inertia in MGP can be estimated to be about 65% of that of a thermal power unit with the same capacity, as shown in Tables II and III [17].

TABLE II
MOMENT OF INERTIA OF A 600 MW THERMAL POWER UNIT

Quality mass	Moment of inertia ($kg{\cdot}m^2$)	Total moment of inertia ($kg{\cdot}m^2$)
Exciter	58.36	22713.22
Generator	7435.81	
Low pressure cylinder	13112.76	
High pressure cylinder	2106.29	

TABLE III
MOMENT OF INERTIA OF A 600 MW MGP

Quality mass	Moment of inertia ($kg{\cdot}m^2$)	Total moment of inertia ($kg{\cdot}m^2$)
Motor exciter	58.36	14988.34
Motor	7435.81	
Generator exciter	58.36	
Generator	7435.81	

The moment of inertia J can be specified by the inertia time constant H:

$$H = \frac{1}{2}\frac{J\omega_0^2}{S_B} \tag{20}$$

where S_B is the rated capacity.

The inertia time H of thermal power units is generally within the range of 2.5∼6.0 s [19]. According to (16), the H of MGP can reach 1.625∼3.9 s for the same rated capacity and rated speed. Therefore, the MGP system can provide enough inertia for power systems with a high proportion of renewable energy to maintain the operation stability.

VII. SIMULATION AND EXPERIMENTAL STUDIES OF MGP ON INERTIAL RESPONSE

A. Simulation of Inertial Support of MGP

In order to test the inertia support of MGP, simulation models are established as shown in Fig. 7. In Model I, there are a 60 MW rated thermal power unit and grid-connected photovoltaic converter, and they are connected to loads through transformers. In Model II, the capacity of the thermal power unit and photovoltaics is the same as in Model I, but photovoltaics are integrated into the grid through MGP.

Figure 8 shows the frequency response curves of Model I in which the PV with converter and Model II in which PV with MGP with 10% load increase at time of 100 s. After the load increase, the PV with MGP has the rate of change of the initial frequency of 0.124 Hz/s, and the frequency nadir is 59.21 Hz, whereas 0.326 Hz/s and 58.94 Hz are for the PV

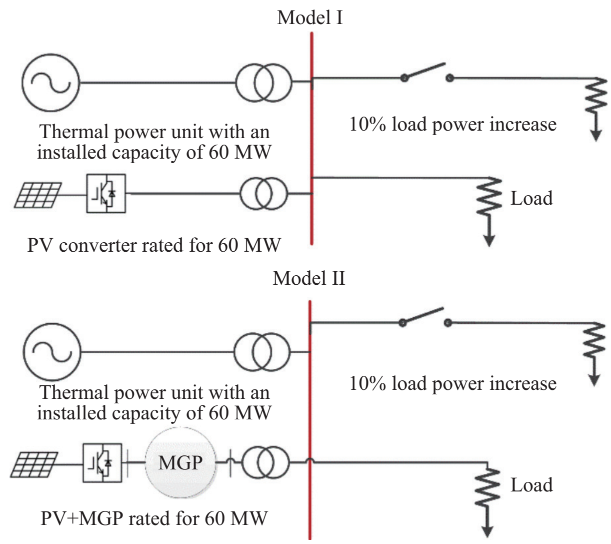

Fig. 7. Simulation model of inertia support of MGP.

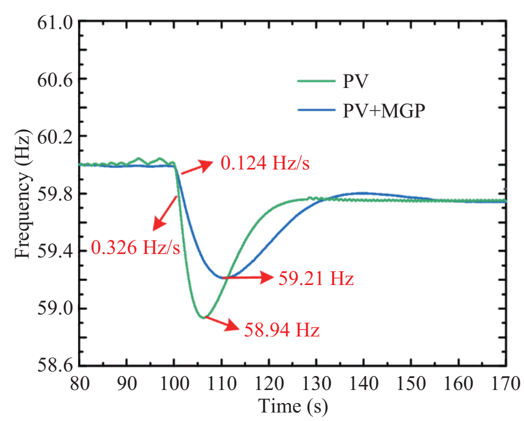

Fig. 8. Frequency response of grid-connected photovoltaic via converter and via MGP.

with a converter. The simulation indicates that Model II has a smaller rate of change and smaller total change than Model I. This means that MGP has provided expected inertia response.

Figure 9 is the active power output for Model I and Model II after the load has a sudden change.

It has been determined that the system frequency decreases after the load increases. One can see from Fig. 9(a) that after load increase, the thermal power unit can instantly give more active power to provide inertial response, but the output power of the PV with a converter remains the same. From Fig. 9(b) for Model II, the PV with MGP can instantaneously provide certain active power to respond to the change of load, because of this power sharing of MGP, the thermal power unit does not need to provide the total imbalanced power at the moment of disturbance. After this first stage of power sharing, the MGP releases its mechanical power to the active power with the time constant of H, so that the MGP's output gradually reduces. During this period, the thermal power unit has already started its primary frequency regulation. This result suggests that MGP can provide inertia support like traditional thermal power units, and sufficient inertial response can be ensured from the large time constant of MGP.

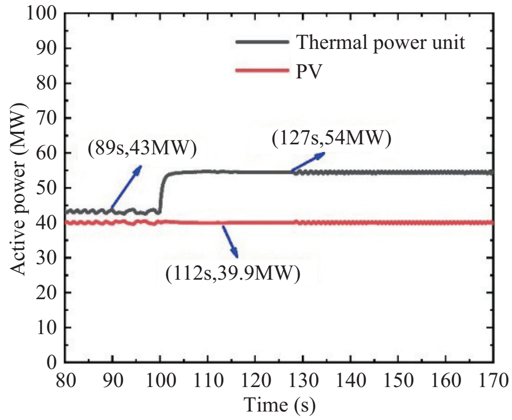

(a) Active power transmitted by thermal power unit and PV with converter after load increase in Model I

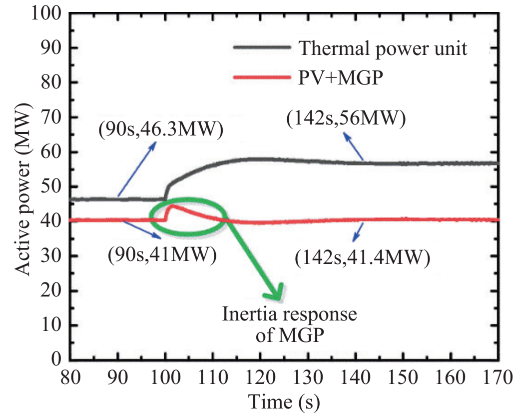

(b) Active power transmitted by thermal power unit and PV with MGP after load increase in Model II

Fig. 9. Active power of model I and model II after load increase.

B. Experimental Study of Inertial Support from MGP

An experimental setup, as shown in Fig. 10, is developed to study the feasibility and effectiveness of MGP for the grid connection of renewable energy.

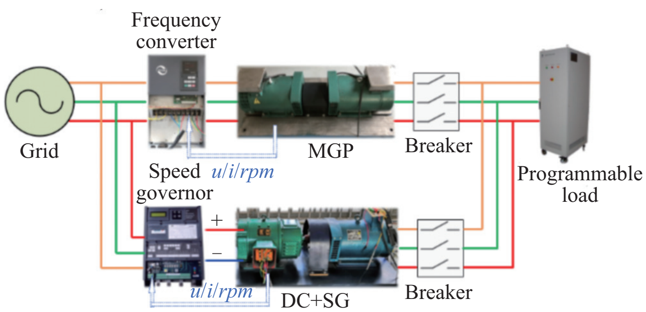

Fig. 10. Experimental platform of MGP.

Due to the limitations of the early stages in experimental studies, motors with only a rating of 5 kW are used, and the converter is powered by a wall plug or PV simulator. This type of setup shows that the MGP system can follow the input power level and transmit the power to the load or back to the wall plug.

The inertial response of MGP is compared with that of a single generator set in this experiment. The setup shown in Fig. 10 has two load operation modes: 1) frequency converter drives the MGP; 2) DC motor drives the SG.

The programmable load is controlled to make a 1500 W load increase, and the frequency response of the generator in two modes after load disturbance are shown in Fig. 11.

Figure 11 demonstrates that MGP has similar inertial responses as traditional SGs. For MGP, the initial change of rate is similar, but the system nadir frequency is clearly smaller, and the frequency oscillation attenuates faster in the recovery process.

In conclusion, MGP can provide actual inertial response to the system. It rebuilds the EM-motion coupling for renewable energy.

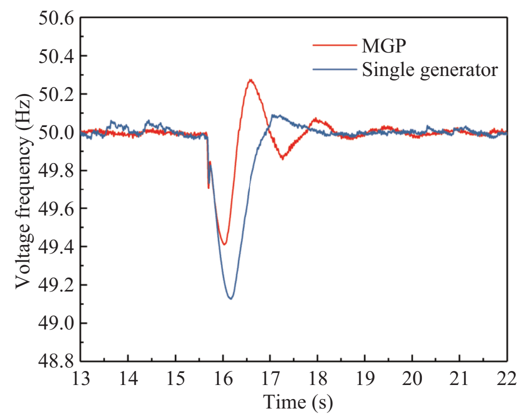

Fig. 11. Frequency response of single generator and MGP after load change.

VIII. Conclusion

This paper explores the theoretical understanding and practical solution to the problem of lack of inertia in power systems with a high proportion of renewable energy. In summary, 1) Obtain a basic conclusion that the nature of the inertia of the synchronous AC grid comes from Lorentz transformation, the inertial response comes from strong electromagnetic-motion coupling. 2) Based on this, it is necessary to understand from the first hypothesis that the inertial response required by the synchronous AC grid may have to be provided by equipment with the coupling. 3) Based on the conclusion, it is necessary to understand from the second hypothesis that the grid-connected converter may be unable to provide the inertial response required by the synchronous AC grid; 4) According to the first hypothesis, the authors suggest it is necessary to rebuild the EM-motion coupling for the electrical power produced by renewable energy. Therefore, the MGP technology with EM-motion coupling is discussed, and studies are made in simulation and experiments.

Acknowledgment

This paper is dedicated to the memory of Dr. Yingkun Zhou, whose pioneering studies are in building the first MGP test stand.

REFERENCES

[1] Y. F. Wen, W. F. Yang, R. H. Wang, W. T. Xu, X. Ye, and T. Li, "Review and prospect of toward 100% renewable energy power systems," *Proceedings of the CSEE*, vol. 40, no. 6, pp. 1843–1855, Mar. 2020.

[2] S. C. Wang, "Current Status of PV in China and Its Future Forecast," *CSEE Journal of Power and Energy Systems*, vol. 6, no. 1, pp. 72–82, Mar. 2020.

[3] Z. Tang, Y. Yang and F. Blaabjerg, "Power electronics: The enabling technology for renewable energy integration," *CSEE Journal of Power and Energy Systems*, vol. 8, no. 1, pp. 39–52, Jan. 2022.

[4] M. Nedd, J. Browell, K. Bell, and C. Booth, "Containing a credible loss to within frequency stability limits in a low-inertia GB power system," *IEEE Transactions on Industry Applications*, vol. 56, no. 2, pp. 1031–1039, Mar./Apr. 2020.

[5] K. V. Vidyanandan and N. Senroy, "Primary frequency regulation by deloaded wind turbines using variable droop," *IEEE Transactions on Power Systems*, vol. 28, no. 2, pp. 837–846, May 2013.

[6] A. P. Hu, B. Yang, P. P. Pan, G. J. Li, Y. B. Tao, and W. Chen, "Study on inertial characteristics of energy storage system with power electronic interface," *Proceedings of the CSEE*, vol. 38, no. 17, pp. 4999–5008, Sep. 2018.

[7] Q. C. Zhong, "Virtual synchronous machines and autonomous power systems," *Proceedings of the CSEE*, vol. 37, no. 2, pp. 336–349, Jan. 2017.

[8] H. D. Sun, B. C. Wang, W. F. Li, C. Yang, W. Wei, and B. Zhao, "Research on inertia system of frequency response for power system with high penetration electronics," *Proceedings of the CSEE*, vol. 40, no. 16, pp. 5179–5192, Aug. 2020.

[9] A. Einstein, "On the electrodynamics of moving bodies," *Annalen der Physik*, vol. 17, no. 10, pp. 891–921, Jan. 1905.

[10] Y. D. Jin, Z. Yu, M. J. Li, and W. J. Jiang, "Comparison of new generation synchronous condenser and power electronic reactive-power compensation devices in application in UHV DC/AC Grid," *Power System Technology*, vol. 42, no. 7, pp. 2095–2102, Jul. 2018.

[11] Z. Q. Li, W. Y. Jiang, Y. B. Wang, W. F. Li, C. K. Li, and Z. L. Xian, "Key technical parameters and optimal design of new types of large capacity synchronous condenser," *Large Electric Machine and Hydraulic Turbine*, no. 4, pp. 15–22, Jul. 2017.

[12] Newfoundland and Labrador Hydro. (2012, Mar.). Review of two generation expansion options for the least-cost supply of power to island interconnected customers for the period 2011–2067, report to government[Online]. Available: https://www.gov.nl.ca/lowerchurchill-project/muskrat_falls_pub_final_report.pdf.

[13] SP Energy. (2019, Dec.). PHOENIX Project Progress Report 2019 [Online]. Available: https://www.spener-gynetworks.co.uk/userfiles/file/Phoenix_Annual_Progress_Report_2019.pdf.

[14] Fraunhofer ISI. (2020, Aug.). Energy Storage in Germany –Present Developments and Applicability in China [Online]. Available: https://www.energypartnership.cn/fileadmin/user_upload/china/media_elements/publications/Energy_Storage_in_Germany_EN_Final.pdf.

[15] S. M. Wei and Y. Z. Huang, "Small signal modeling and damping characteristic of MGP for wind power integration," *Automation of Electric Power Systems*, vol. 41, no. 22, pp. 16–25, Nov. 2017.

[16] S. M. Wei, Y. K. Zhou, G. R. Xu, and Y. Z. Huang, "Motor-generator pair: a novel solution to provide inertia and damping for power system with high penetration of renewable energy," *IET Generation, Transmission & Distribution*, vol. 11, no. 7, pp. 1839–1847, May 2017.

[17] S. M. Wei, Y. K. Zhou, S. Li, and Y. Z. Huang, "A possible configuration with motor-generator pair for renewable energy integration," *CSEE Journal of Power and Energy Systems*, vol. 3, no. 1, pp. 93–100, Mar. 2017.

[18] S. J. Cheng, Y. J. Cao, and Q. Y. Jiang, *Theory and Method of Subsynchronous Oscillation in Power System*, Beijing: Science Press, 2009.

[19] P. Kundur, Power System Stability and Control, New York: McGraw-Hill, 1994.

Yongzhang Huang (M'16) received a Ph.D degree from the Institute of High Energy Physics of the Chinese Academy of Science in 1991. He had been involved in working on high energy particle accelerators and semiconductor equipment.

He is currently a professor with the School of Electrical and Electronics Engineering, North China Electric Power University. He is also the Deputy Director of the State Key Laboratory of Alternate Electrical Power System with Renewable Energy Sources.

His current research interests include: instability of power systems with high proportion renewable energy, reliability testing equipment for power semiconductor device.

Yuxuan Wang received a B.S degree in Automation from Yichun College, Yichun, Jiangxi, China, in 2013 and a M.S degree in Electrical Engineering from North China Electric Power University, Beijing, China, in 2017. He is currently pursuing a Ph.D. degree in Electrical Engineering at North China Electric Power University.

His research interests include renewable energy systems analysis, integrated energy systems, energy forecasting, and deep reinforcement learning.

Chenyang Li (S'18) received a B.S. degree in Electrical Engineering and automation from North China Electric Power University (NCEPU), Baoding, China, in 2014. He is currently pursuing a Ph.D. degree in Electrical Engineering at NCEPU, Beijing, China.

His research interests primarily include the stability of power systems with renewable energy, and control of power electronics.

Haisen Zhao received the B.E. in Agricultural Electrification and Automation from the Agriculture University of Hebei, Baoding, China, in 2004. He received his M.E. and Ph.D. in Electric Machines and apparatus from North China Electric Power University (NCEPU), Beijing, China, in 2007, and in 2011, respectively.

He is currently a professor with the School of Electrical and Electronic Engineering, North China Electric Power University. He is also a fellow of the Institute of Engineering and Technology (IET). Dr. Zhao is the author and co-author of more than 100 articles in peer-reviewed journals and major international conferences. Furthermore, he has 20 patents awarded in the area of electric machine design, control, and energy-saving technologies. His research interests include motor design and fault diagnosis, energy-saving technologies of electric machines and drive systems, stability analysis of power system with renewable energy, and wireless power transfer.

Qianyu Wu (S'18) received a B.E. degree in Electrical Engineering and automation and a M.E. degree in Power Systems and Automation from the North China Electric Power University (NCEPU), Beijing, China, in 2015 and 2018, respectively, where she is currently pursuing a Ph.D. degree with the School of Electrical and Electronic Engineering.

Her research interests primarily include the stability of power systems with renewable energy.